

This copy is for your personal, non-commercial use only.

If you wish to distribute this article to others, you can order high-quality copies for your colleagues, clients, or customers by [clicking here](#).

Permission to republish or repurpose articles or portions of articles can be obtained by following the guidelines [here](#).

The following resources related to this article are available online at
www.sciencemag.org (this information is current as of February 28, 2011):

Updated information and services, including high-resolution figures, can be found in the online version of this article at:

<http://www.sciencemag.org/content/331/6020/1081.full.html>

Supporting Online Material can be found at:

<http://www.sciencemag.org/content/suppl/2011/02/23/331.6020.1081.DC1.html>

A list of selected additional articles on the Science Web sites related to this article can be found at:

<http://www.sciencemag.org/content/331/6020/1081.full.html#related>

This article cites 29 articles, 10 of which can be accessed free:

<http://www.sciencemag.org/content/331/6020/1081.full.html#ref-list-1>

This article has been cited by 1 articles hosted by HighWire Press; see:

<http://www.sciencemag.org/content/331/6020/1081.full.html#related-urls>

This article appears in the following subject collections:

Molecular Biology

http://www.sciencemag.org/cgi/collection/molec_biol

Translation-Independent Localization of mRNA in *E. coli*

Keren Nevo-Dinur, Anat Nussbaum-Shochat, Sigal Ben-Yehuda, Orna Amster-Choder*

Understanding the organization of a bacterial cell requires the elucidation of the mechanisms by which proteins localize to particular subcellular sites. Thus far, such mechanisms have been suggested to rely on embedded features of the localized proteins. Here, we report that certain messenger RNAs (mRNAs) in *Escherichia coli* are targeted to the future destination of their encoded proteins, cytoplasm, poles, or inner membrane in a translation-independent manner. Cis-acting sequences within the transmembrane-coding sequence of the membrane proteins are necessary and sufficient for mRNA targeting to the membrane. In contrast to the view that transcription and translation are coupled in bacteria, our results show that, subsequent to their synthesis, certain mRNAs are capable of migrating to particular domains in the cell where their future protein products are required.

Targeting of specific mRNAs to different subcellular domains is generally believed to occur only in eukaryotes, where the synthesis and processing of mRNA is compartmentalized between nucleus and cytoplasm (1–3). In bacteria, gene transcription and translation are not thought to be compartmentalized, and conventional wisdom holds that translation is coupled to mRNA synthesis (4). Consequently, protein localization is believed to be governed by intrinsic features of proteins and not of their mRNA transcripts (5–7). Accordingly, several bacterial mRNAs have been shown to localize near the site of their synthesis on the genome (8). On the other hand, the transcription machinery and the ribosomes occupy different subcellular regions within different bacterial cells (9, 10), raising the possibility that mature mRNAs can move from the nucleoid to other cellular sites where they are translated. Here, we report the existence of bacterial mechanisms for subcellular protein localization that operate at the level of mRNA targeting in a translation-independent manner.

We followed the location of *cat* and *lacY* transcripts, encoding the cytoplasmic chloramphenicol acetyltransferase and the membrane-bound lactose permease, respectively (11, 12), in living *Escherichia coli* cells by cloning six copies of the binding sequence of phage MS2 coat protein (6xbs) upstream of these genes. We visualized the resulting 6xbs-tagged *cat* and *lacY* transcripts (*cat*_{6xbs} and *lacY*_{6xbs}, respectively) by fluorescence microscopy in cells expressing the MS2 coat protein fused to green fluorescent protein (MS2-GFP) (fig. S1) (13). We observed the *cat* transcripts in the cytoplasm in a helixlike pattern (Fig. 1A, a, and fig. S2), reminiscent of the helical RNA structures documented previously in *E. coli* (14).

In contrast, we detected *lacY* transcripts preferentially at or near the cytoplasmic membrane (Fig. 1A, b). In cells lacking 6xbs-tagged transcripts, MS2-GFP was evenly distributed throughout the cytoplasm (Fig. 1A, c), whereas the distribution of short transcripts, composed of the 6xbs, was similar to *cat* (fig. S3). We also examined the subcellular localization of *cat* and *lacY* transcripts by cellular fractionation followed by reverse transcription and polymerase chain reaction amplification (RT-PCR), resulting in the detection of *cat* and *lacY* transcripts in the cytosolic and membrane fractions, respectively (Fig. 1B, a and b). We used real-time PCR to quantify the enrichment in *cat* and *lacY* transcripts in the cytosolic and membrane fractions, respectively (fig. S4). Taken together, each of these transcripts localizes to the compartment where its protein product functions.

To examine the subcellular localization of transcripts of an operon that encodes both membrane and soluble proteins, we introduced the 6xbs in various locations within the *bgl* operon of *E. coli* that encodes the BglG transcription factor, the BglF membrane-bound sugar permease, and the soluble phospho-β-glucosidase, BglB. We then confirmed functionality of all 6xbs-tagged transcripts [see supporting online material (SOM) (15)]. When the 6xbs were introduced immediately upstream of the chromosomal *bglF* gene, the MS2-GFP protein was observed at the cell membrane (Fig. 1A, d). In contrast, when the chromosomal *bglF* gene was replaced by *cat*_{6xbs}, the MS2-GFP displayed a helical, away-from-the-membrane distribution, the same as that of plasmid-encoded *cat* (Fig. 1A, e). We noticed localization patterns similar to the ones obtained in live cells when we used fluorescence *in situ* hybridization (FISH) to detect *bglF* and *cat* transcripts (Fig. 1D and fig. S5). To examine the correlation between the localization of the *bglF* transcript and the BglF protein, mCherry was fused to *bglF*_{6xbs}. We observed the BglF-mCherry fusion protein around the cell membrane (Fig. 1C, b), which is similar to the MS2-GFP localization pattern (Fig. 1C, a and c) and different

from the localization of mCherry mRNA and protein when not fused to BglF (fig. S6). In fact, all truncated transcripts of the *bgl* operon that included *bglF* localized to the membrane (Fig. 1A, g, h, j, and k), including transcripts of *bglF* expressed as a monocistron (Fig. 1A, f). This pattern of localization did not depend on whether the 6xbs were introduced adjacent to *bglF* (Fig. 1A, f, g, and j), *bglB* (Fig. 1A, h), or *bglG* (Fig. 1A, k). However, transcripts expressing only the soluble BglB protein were distributed similarly to *cat* transcripts (Fig. 1A, i), whereas those containing only the *bglG* gene were detected near the poles (Fig. 1A, l), similar to the localization pattern of the BglG protein in cells not expressing BglF (16). Cellular fractionation followed by RT-PCR confirmed that all transcripts containing the membrane protein-encoding *bglF* gene localized to the membrane, whereas transcripts encoding only the soluble BglB protein were present in the cytosol, and those encoding the polar BglG were detected in the membrane and in the cytosolic fractions (Fig. 1B, c to k). Thus, localization of the monocistronic transcripts of each *bgl* gene correlates with subsequent localization of the respective protein products. However, the membrane-encoding cistron is dominant to the hydrophilic-encoding cistron in determining localization of multicistronic mRNAs. Conversely, a bicistronic mRNA, which consists of *bglG* and *cat*_{6xbs}, exhibited the localization pattern of both partners—that is, helical with accumulation near the poles (Fig. 1A, m, and fig. S7, a to c).

To determine if targeting is a property of the mRNA, we uncoupled transcription and translation by treating the cells with vast excess of kasugamycin or chloramphenicol, which inhibit initiation or elongation of translation, respectively (17, 18). These treatments resulted in complete inhibition of *bglF* mRNA translation (fig. S8), but did not affect targeting of *bglF* transcripts to the membrane (Fig. 2, B and F). Treatment with each antibiotic had no effect on the distribution of MS2-GFP itself (Fig. 2, A and E). Chloramphenicol was reported to slightly increase stability of certain mRNAs (19), but we saw no substantial difference in the half-life of *bglF* transcripts in treated and untreated cells (fig. S9). Of note, the half-life of *bglF* transcripts is shorter than that of most *E. coli* mRNAs (20) and considerably shorter than the duration of treatment with both antibiotics. Hence, most, if not all, *bglF* transcripts observed after antibiotic treatment were new untranslated transcripts. Treatment with the transcription-inhibiting drug rifampicin, with or without kasugamycin or chloramphenicol, resulted in a lack of *bglF*_{6xbs} transcripts and, hence, in even spreading of MS2-GFP molecules in the cell (fig. S10). The distribution of *bglF*_{6xbs} or *cat*_{6xbs} transcripts was also not affected by the translation-inhibiting antibiotics (Fig. 2, C, D, and G, and fig. S11). Therefore, these mRNAs seem to harbor the information that determines their nonrandom localization in the cell by a

Department of Microbiology and Molecular Genetics, Institute for Medical Research Israel-Canada, The Hebrew University Faculty of Medicine, Post Office Box 12272, Jerusalem 91120, Israel.

*To whom correspondence should be addressed. E-mail: amster@cc.huji.ac.il

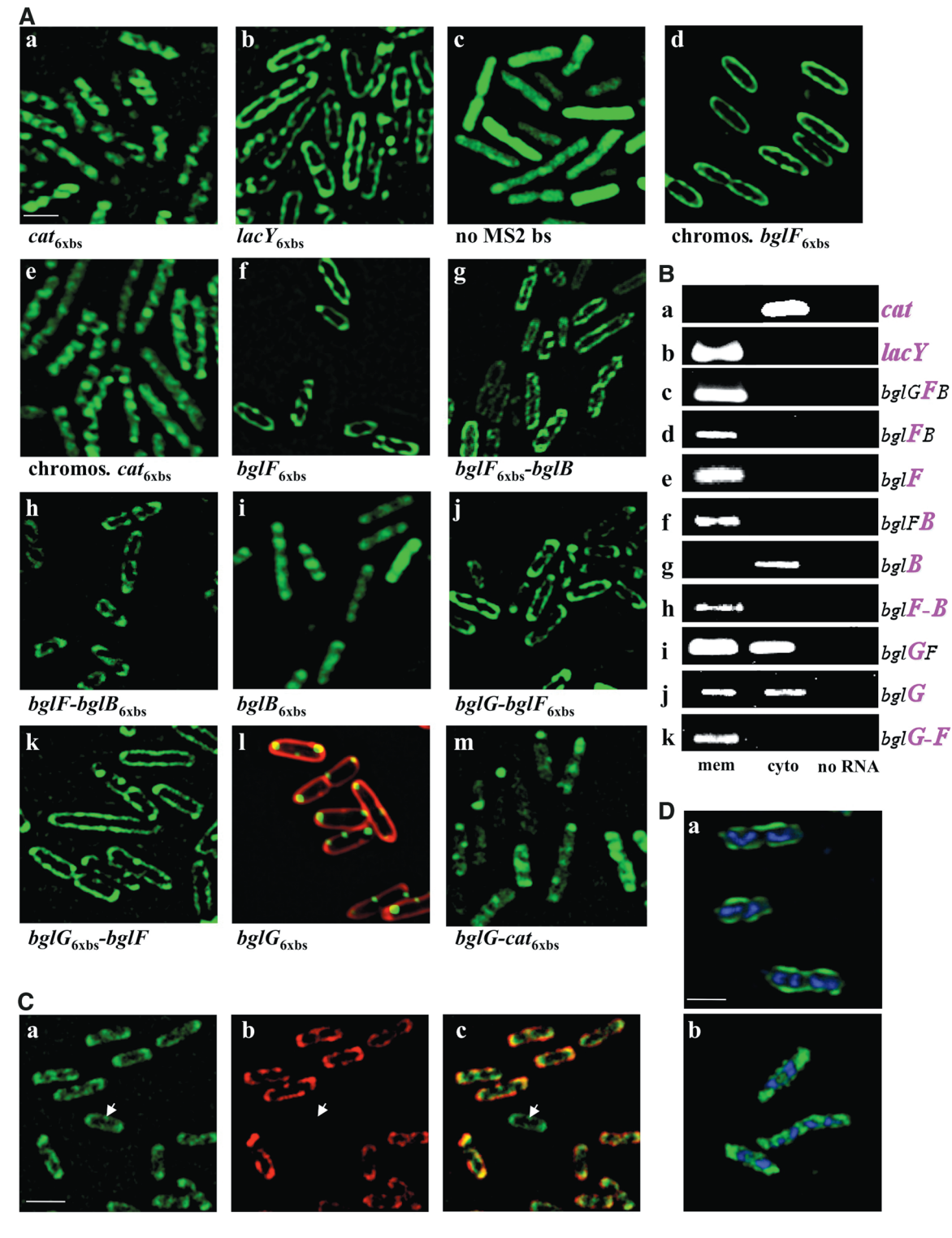
translation-independent mechanism. To reinforce this conclusion, we aimed at uncoupling transcription and translation by a different approach. Mutating the first codon of *bglF* yielded transcripts that were targeted to the membrane (Fig. 3A), but some translation from a downstream start codon was detected (fig. S12). To complete-

ly inhibit protein synthesis, we introduced a “5'-translational blockage” (21), which consisted of 12 consecutive rare leucine codons, near the 5' end of the *bglF* gene. The resultant transcript was readily detected by RT-PCR, but as expected, its translation was blocked (fig. S13). Noticeably, this untranslated *bglF* mRNA was

viewed near the membrane (Fig. 3B), demonstrating once again that membrane recruitment of the mRNA is translation-independent.

To characterize the mRNA element that targets *bglF* transcripts to the membrane, we fused the 6xbs to truncated *bglF* derivatives that encode either the hydrophilic IIB^{bgl} domain or the

Fig. 1. Subcellular localization of mRNA transcripts correlates with subsequent localization of their protein products. (A) Fluorescence microscopy images of cells expressing MS2-GFP (green) and transcripts containing or lacking binding sites for MS2-GFP. “6xbs” after a gene's name denotes that the MS2 binding sites were introduced immediately next to this gene. Cells shown in (I) were supplemented with the fluorescent membrane stain FM4-64. Transcripts were plasmid-encoded, unless otherwise stated. Scale bar, 1 μm. (B) Cells deleted for the *bgl* operon and transformed with plasmids encoding the genes listed on the right were fractionated as described in the SOM (see fig. S17 for verification of successful fractionation) (15). Transcripts, expressed as mono- or multicistronic, present in the different fractions were monitored by RT-PCR. Purple indicates those genes whose sequence was amplified. In (h) and (k), the junction region between the genes in purple was amplified. mem, membrane; cyto, cytosol. (C) (a and b) Fluorescence microscopy images of cells expressing MS2-GFP (green) and a BglF-mCherry fusion protein (red), whose transcript contains the 6xbs. (c) An overlay of the signals. Scale bar, 1 μm. The possibility of false detection due to fluorescence leakage between the filters was ruled out. The white arrows point at a cell in which the 6xbs-tagged *bglF*-mCherry transcripts



are detected (a) and the BglF-mCherry protein is not (b) (see also the results in fig. S18). (D) Chromosome-encoded *bglF*_{6xbs} (a) or *cat*_{6xbs} (b) transcripts were detected by FISH, as described in the SOM (15), and DNA was stained with 4',6-diamidino-2-phenylindole (see fig. S5) (15). Scale bar, 1 μm.

Fig. 2. Transcripts localization is not affected by inhibition of translation. (**A** to **G**) Fluorescence microscopy images of cells expressing the MS2-GFP protein (green) and *bglG-bglF* transcripts lacking binding sites for MS2-GFP [(**A**) and (**E**)], *bglG-bglF*_{6xbs} [(**B**) and (**F**)], *bglG*_{6xbs} [(**C**) and (**G**)], or *cat*_{6xbs} (**D**) transcripts. The cells were treated for 10 min with 10 mg/ml kasugamycin [(**A**) to (**D**)] or 250 µg/ml chloramphenicol [(**E**) to (**G**)] before microscopy. Scale bar, 1 µm.

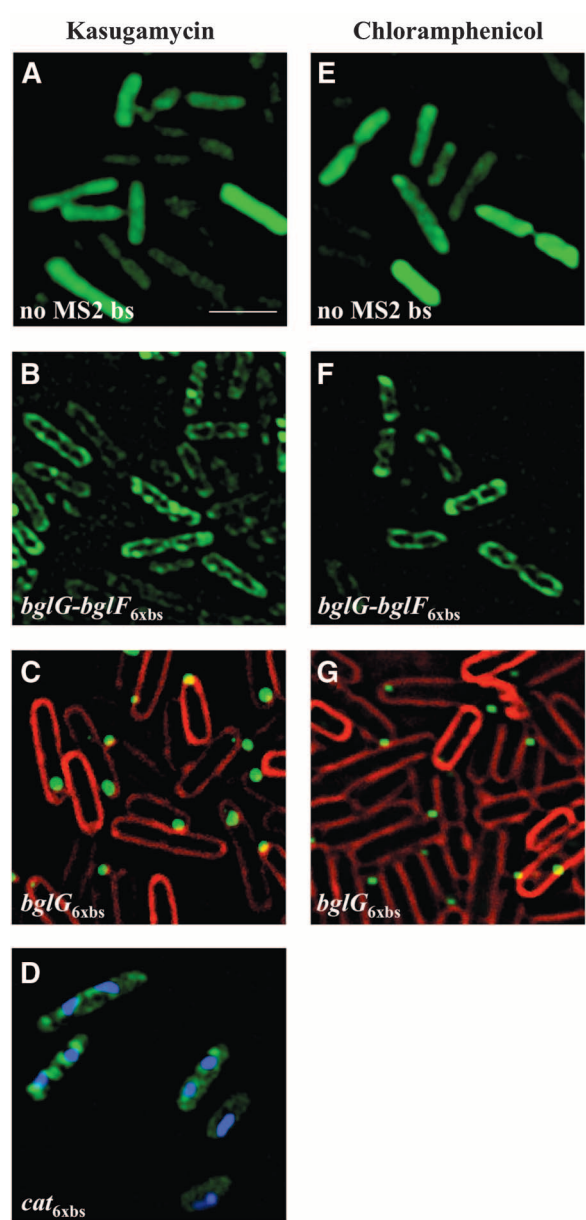
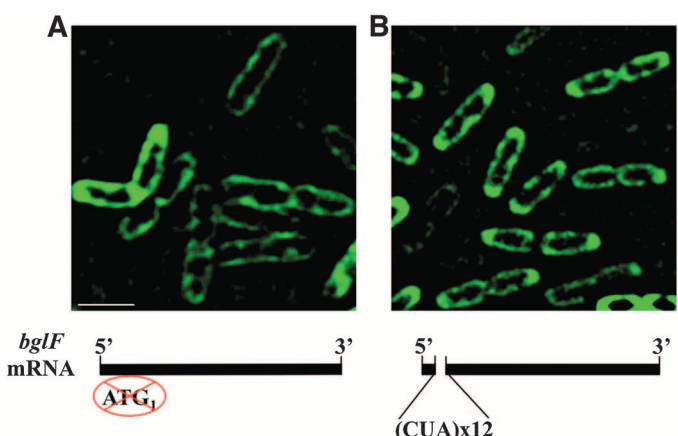


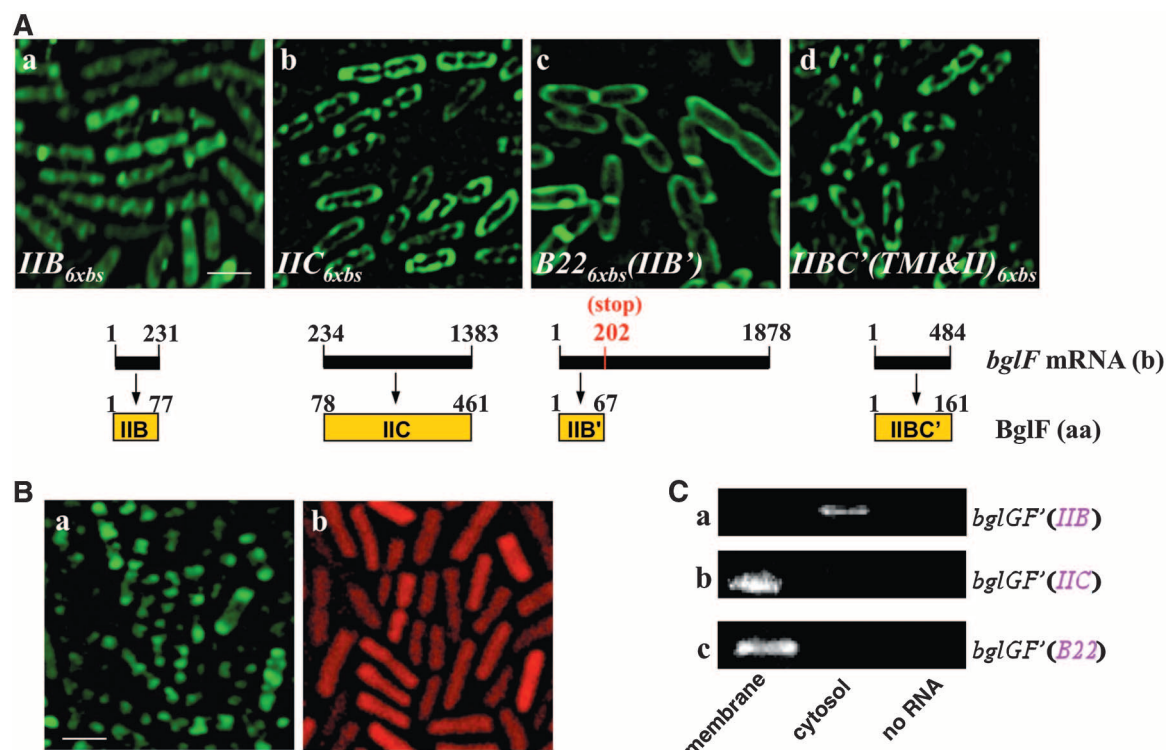
Fig. 3. Membrane localization of *bglF* transcripts is not affected by translational blockage. Fluorescence microscopy images of cells expressing the MS2-GFP protein (green) and 6xbs-tagged transcripts of *bglF* alleles, which have either a mutated start codon (**A**) or 12 consecutive rare leucine codons (CUA) near the 5' end (**B**). Scale bar, 1 µm.



hydrophobic IIC^{bgl} domain [designated the B and C domains, respectively, hereafter (22)] and followed their subcellular localization. Transcripts encoding the soluble B domain were observed in the cytoplasm (Fig. 4A, a), in accord with localization of the encoded protein (Fig. 4B), whereas those encoding the membrane C domain were detected at the membrane (Fig. 4A, b). Therefore, the membrane-targeting information is located within the sequence that encodes the membrane-spanning domain. Transcripts of a *bglF*_{6xbs} variant that contains a stop codon before the end of the first domain, thereby yielding a full-length *bglF* transcript that encodes only the soluble B domain (termed B22; fig. S14), were observed at the membrane (Fig. 4A, c), substantiating the notion that the cis-acting sequence for membrane targeting is contained within the transcript. RT-PCR after cell fractionation confirmed the microscopy observations (Fig. 4C). Taken together, targeting of *bglF* transcripts to the membrane requires the region that encodes the membrane domain, but translation of this region is not necessary. Further dissection of the sequences required for transcripts localization demonstrated that the sequence encoding the first two transmembrane helices of BglF is sufficient for membrane targeting of the transcripts (Fig. 4A, d), whereas the region encoding the N-terminal RNA-binding domain of BglG is sufficient for mRNA polar targeting (fig. S7, d to f).

The results presented here show that mechanisms for targeting mRNAs to subcellular locations, where their protein products are required, exist in bacteria. Previously, mRNA features were proposed to be involved in targeting proteins to the type III secretion system in Gram-negative bacteria (23). mRNA targeting might be tied to processes other than localized translation, for instance, mRNA degradation. The latter possibility is in accord with previous reports showing that components of the *E. coli* mRNA degradosome associate with the membrane and assemble into helical filaments (24, 25). Our study also establishes the existence of a translation-independent RNA transport mechanism in bacteria. By and large, mRNA localization can be achieved by facilitated diffusion in the cytoplasm or by active transport along cytoskeletal filaments (26, 27). The short half-life of the *bglF* transcripts suggests that an active mechanism is involved in targeting them to the membrane. The finding of inner membrane-bound ribosomes in *E. coli*, which are actively engaged in translation (28), indicates that the set-up for translation of transcripts that encode membrane proteins exists. Regarding the zip codes that target mRNAs to the membrane, a recent analysis suggested that uracils, which are highly represented in transcripts that encode integral membrane proteins, might serve as a physiologically relevant signature to this group of mRNAs (29). This evolutionarily conserved U richness might serve as a zip code that attracts proteins, including ribosomal proteins, which bring the transcripts to the mem-

Fig. 4. Membrane localization of *bglF* transcripts requires the membrane domain-encoding sequence. (A) Fluorescence microscopy images of cells expressing the MS2-GFP protein (green) and 6xbs-tagged truncated *bglF* transcripts encoding: (a) the soluble B domain; (b) the membrane-bound C domain; (c) the mutant B22 allele, which yields a full-length transcript but a truncated B domain due to a stop codon; and (d) the B domain and the first two transmembrane helices of the C domain. The *bglF* transcripts and their respective protein products are schematically shown. stop, stop codon; b, bases; aa, amino acids. Scale bar, 1 μ m. (B) Fluorescence microscopy images of cells expressing MS2-GFP (green) and the B domain of BglF fused to mCherry (red), whose transcript contains the 6xbs. Scale bar, 1 μ m. (C) Cell fractionation and detection of transcripts by RT-PCR as described in Fig. 1B. (a), (b), and (c) are as in (A). The *bglF* sequence amplified in each case is in purple.



brane. Indeed, an mRNA encoding the rhomboid 1 transmembrane protein from *Drosophila melanogaster* still localized predominantly to the membrane in *E. coli* cells (fig. S15). Finally, our results imply that mRNA targeting is in tight correlation with the requirements for complex formation. Specifically, *bglG* mRNA is targeted to the membrane or to the poles, depending on whether it is expressed with or without *bglF*, respectively. This is in full agreement with the localization of the BglG protein, which associates with BglF at the membrane (30) or with the general PTS proteins at the poles (16), depending on environmental conditions.

References and Notes

1. E. Lécyer *et al.*, *Cell* **131**, 174 (2007).
2. D. St. Johnston, *Nat. Rev. Mol. Cell Biol.* **6**, 363 (2005).
3. C. E. Holt, S. L. Bullock, *Science* **326**, 1212 (2009).
4. I. Iost, M. Dreyfus, *EMBO J.* **14**, 3252 (1995).
5. A. Janakiraman, M. B. Goldberg, *Trends Microbiol.* **12**, 518 (2004).
6. G. Ebersbach, C. Jacobs-Wagner, *Trends Microbiol.* **15**, 101 (2007).
7. L. Shapiro, H. H. McAdams, R. Losick, *Science* **326**, 1225 (2009).
8. P. Montero Llopis *et al.*, *Nature* **466**, 77 (2010).
9. P. J. Lewis, S. D. Thaker, J. Errington, *EMBO J.* **19**, 710 (2000).
10. T. A. Azam, S. Hiraga, A. Ishihama, *Genes Cells* **5**, 613 (2000).
11. M. W. Chen, V. Nagarajan, *J. Bacteriol.* **175**, 5697 (1993).
12. L. Guan, H. R. Kaback, *Annu. Rev. Biophys. Biomol. Struct.* **35**, 67 (2006).
13. I. Golding, E. C. Cox, *Proc. Natl. Acad. Sci. U.S.A.* **101**, 11310 (2004).
14. M. Valencia-Burton *et al.*, *Proc. Natl. Acad. Sci. U.S.A.* **106**, 16399 (2009).
15. Materials and methods, as well as other supporting material, are available on *Science Online*.
16. L. Lopian, Y. Elisha, A. Nussbaum-Shochat, O. Amster-Choder, *EMBO J.* **29**, 3630 (2010).
17. F. Schluenzen *et al.*, *Nat. Struct. Mol. Biol.* **13**, 871 (2006).
18. A. S. Weisberger, *Annu. Rev. Med.* **18**, 483 (1967).
19. U. Lundberg, G. Nilsson, A. von Gabain, *Gene* **72**, 141 (1988).
20. J. A. Bernstein, A. B. Khodursky, P. H. Lin, S. Lin-Chao, S. N. Cohen, *Proc. Natl. Acad. Sci. U.S.A.* **99**, 9697 (2002).
21. E. Goldman, A. H. Rosenberg, G. Zubay, F. W. Studier, *J. Mol. Biol.* **245**, 467 (1995).
22. O. Amster-Choder, *Curr. Opin. Microbiol.* **8**, 127 (2005).
23. J. A. Sorg, N. C. Miller, O. Schnewind, *Cell. Microbiol.* **7**, 1217 (2005).
24. A. Taghbalout, L. Rothfield, *Proc. Natl. Acad. Sci. U.S.A.* **104**, 1667 (2007).
25. V. Khemici, L. Poljak, B. F. Luisi, A. J. Carpousis, *Mol. Microbiol.* **70**, 799 (2008).
26. K. Czapinski, R. H. Singer, *Trends Biochem. Sci.* **31**, 687 (2006).
27. I. M. Palacios, *Semin. Cell Dev. Biol.* **18**, 163 (2007).
28. A. A. Herskovits, E. Bibi, *Proc. Natl. Acad. Sci. U.S.A.* **97**, 4621 (2000).
29. J. Prilusky, E. Bibi, *Proc. Natl. Acad. Sci. U.S.A.* **106**, 6662 (2009).
30. L. Lopian, A. Nussbaum-Shochat, K. O'Day-Kerstein, A. Wright, O. Amster-Choder, *Proc. Natl. Acad. Sci. U.S.A.* **100**, 7099 (2003).
31. We acknowledge members of S.B.-Y.'s group for help with fluorescence microscopy, members of O.A.-C.'s group for stimulating discussions, and E. Bibi and E.S. Bochkareva for technical advice on cell fractionation. We thank the following individuals for their gifts: I. Golding for pIG-K33, R. H. Singer for pSL-MS2 6, and Z. Livneh for purified single-stranded DNA binding protein (SSB) and anti-SSB serum. We are grateful to A. Wright, E. Bibi, and R. Losick for critically reading our manuscript. This research was supported by a research grant (awarded to O.A.-C.) by the Israel Science Foundation founded by the Israel Academy of Sciences and Humanities. S.B.-Y. is supported by the European Research Council starting grant (209130).

Supporting Online Material

www.sciencemag.org/cgi/content/full/331/6020/1081/DC1
Materials and Methods
Figs. S1 to S18
Table S1
References

27 July 2010; accepted 13 January 2011
10.1126/science.1195691